arXiv:1406.6776v3 [hep-ph] 10 Oct 2014

Precise determination of Z-Z' mixing at the CERN LHC

V. V. Andreev,[a,*] P. Osland,[b,†] A. A. Pankov[c,‡]

[a] *The F. Scorina Gomel State University, 246019 Gomel, Belarus*

[b] *Department of Physics and Technology,*

University of Bergen, Postboks 7803, N-5020 Bergen, Norway

[c] *The Abdus Salam ICTP Affiliated Centre,*

Technical University of Gomel, 246746 Gomel, Belarus

(Dated: October 13, 2014)

Abstract

We discuss the expected sensitivity to Z' boson effects in the $W^{\pm}$ boson pair production process at the Large Hadron Collider (LHC). The results of a model-dependent analysis of Z' boson effects are presented as constraints on the Z-Z' mixing angle ϕ and Z' boson mass. The process $pp \to W^+W^- + X$ allows to place stringent constraints on the Z-Z' mixing angle. Specifically, we find that the present LHC bounds on the mixing angle are of the order a few times 10^{-3}, what is of the same order as those derived from the electroweak data. These results were derived from analysis of W-pair production at $\sqrt{s} = 8$ TeV and integrated luminosity of 20 fb^{-1}. Further improvement on the constraining of this mixing can be achieved from the analysis of data on $WW \to l\nu l'\nu'$ ($l, l' = e$ or μ) and $WW \to l\nu jj$ final states collected at the LHC with nominal energy and luminosity, 14 TeV and 100 fb^{-1}, and should be $\phi \sim 10^{-4} - 10^{-3}$.

PACS numbers: 12.60.-i, 12.60.Cn, 14.70.Fm, 29.20.Ej

* quarks@gsu.by

† per.osland@ift.uib.no

‡ pankov@ictp.it

I. INTRODUCTION

Nearly all electroweak and strong-interaction data are well described by the standard model (SM) [1]. However, there are many reasons why this is not believed to be the ultimate theory. Grand Unified Theories (GUT), possibly together with Supersymmetry, which allows a successful unification of the three gauge coupling constants at the high scale, are among the main candidates for new and richer physics. Many of these GUTs, including superstring and left-right-symmetric models, predict the existence of new neutral gauge bosons, which might be light enough to be accessible at current and/or future colliders [2–5].

The search for these Z' particles is an important aspect of the experimental physics program of current and future high-energy colliders. Present limits from direct production at the LHC and virtual effects at LEP, through interference or mixing with the Z boson, imply that new Z' bosons are rather heavy and mix very little with the Z boson. Depending on the considered theoretical model, Z' masses of the order of 2.5–3.0 TeV [6–9] and Z-Z' mixing angles at the level of a few per mil are excluded [10–12]. The size of the mixing angle is strongly constrained by very high precision Z-pole experiments at LEP and the SLC [13]. They contain measurements from the Z line shape, from the leptonic branching ratios normalized to the total hadronic Z decay width and from leptonic forward-backward asymmetries. A Z' boson, if lighter than about 5 TeV, could be discovered at the LHC [14, 15] with $\sqrt{s} = 14$ TeV in the Drell-Yan process

$$pp \to Z' \to \ell^+\ell^- + X \tag{1}$$

with $\ell = e, \mu$. The future e^+e^- International linear collider (ILC) with high c.m. energies and longitudinally polarized beams could indicate the existence of Z' bosons via its interference effects in fermion pair production processes, with masses up to about $6 \times \sqrt{s}$ [16] while Z-Z' mixing will be constrained down to $\sim 10^{-4} - 10^{-3}$ in the process $e^+e^- \to W^+W^-$ [17, 18].

After the discovery of a Z' boson at the LHC via the process (1), some diagnostics of its couplings and Z-Z' mixing needs to be done in order to identify the correct theoretical framework. In this paper we study the potential of the LHC to discover Z-Z' mixing effects in the process

$$pp \to W^+W^- + X \tag{2}$$

and compare it with that expected at the ILC.

The $W^{\pm}$ boson pair production process (2) is rather important for studying the electroweak gauge symmetry at the LHC. Properties of the weak gauge bosons are closely related to electroweak symmetry breaking and the structure of the gauge sector in general. In addition, the diboson decay modes of Z' directly probe the gauge coupling strength between the new and the standard-model gauge bosons. The coupling strength strongly influences the decay branching ratios and the natural widths of the new gauge bosons. Thus, detailed examination of the process (2) will both test the gauge sector of the SM with the highest accuracy and throw light on New Physics (NP) that may appear beyond the SM.

Direct searches for a heavy WW resonance have been performed by the CDF and D0 collaborations at the Tevatron. The D0 collaboration explored diboson resonant production using the $\ell\nu\ell'\nu'$ and $\ell\nu jj$ final states [19]. The CDF collaboration also searched for resonant WW production in the $e\nu jj$ final state, resulting in a lower limit on the mass of an RS graviton, Z' and W' bosons [12].

The direct WW resonance search by the ATLAS Collaboration using $l\nu l'\nu'$ final-state events in 4.7 fb^{-1} pp collision data at the collider energy of 7 TeV set mass limits on such resonances [20, 21]. Also, the $l\nu jj$ final state allows to reconstruct the invariant mass of the system, under certain assumptions on the neutrino momentum from a W boson decay.

In this note, we examine the feasibility of observing a Z' boson in the $W^{\pm}$ pair production process at the LHC, which in contrast to the Drell-Yan process (1) is not the principal discovery channel, but can help to understand the origin of new gauge bosons. In the scenarios that we will consider in the following, the mechanism of Z' production and subsequent decay to WW is directly proportional to the Z-Z' mixing. Also, we show that the sensitivity of the $W^{\pm}$ pair production process in their pure leptonic decay channels to the Z-Z' mixing angle at the LHC with 8 TeV allows to place limits on the mixing angle that are complementary to those derived from the current electroweak data, whereas the increasing LHC energy and time-integrated luminosity up to their planned values allow to get corresponding limits that are competitive to the current ones and to those expected from future ILC data.

The paper is organized as follows. In Section II, we briefly review models involving additional Z' bosons and emphasize the role of Z-Z' mixing in the process (2). In Section III we give expressions for basic observables, as well as formulae for helicity amplitudes of the process under consideration. In Section IV we discuss signals and backgrounds, both for the $ee, \mu\mu$ and for the $e\mu$ cases, and in Section V we discuss achievable constraints on Z' models.

Section VI presents some concluding remarks.

II. Z' MODELS

There are many theoretical models which predict a Z' with mass possibly in the TeV range. Popular classes of models are represented by E_6-motivated models, the Left-Right Symmetric Model (LR), the Z' in an 'alternative' left-right scenario and the Sequential Standard Model (SSM), which has a heavier boson with couplings like those of the SM Z. Searching for Z' in the above models has been widely studied in the literature [2–4] and applied at LEP2, the Tevatron and the LHC. For the notation we refer to [17], where also a brief description can be found. The different models considered are: (i) Models related to the breaking of E_6, parametrized by a parameter β, familiar cases are the Z'_χ, Z'_ψ, Z'_η and Z'_I models; (ii) Left-right models, originating from the breaking down of an $SO(10)$ grand-unification symmetry, leading to a $Z'_{\rm LR}$; (iii) The sequential $Z'_{\rm SSM}$, which has couplings to fermions being the same as those of the SM Z.

The mass-squared matrix of the Z and Z' can have non-diagonal entries δM^2, which are related to the vacuum expectation values of the fields of an extended Higgs sector:

$$M^2_{ZZ'} = \begin{pmatrix} M_Z^2 & \delta M^2 \\ \delta M^2 & M_{Z'}^2 \end{pmatrix} . \tag{3}$$

Here, Z and Z' denote the weak gauge boson eigenstates of $SU(2)_L \times U(1)_Y$ and of the extra $U(1)'$, respectively. The mass eigenstates, Z_1 and Z_2, diagonalizing the matrix (3), are then obtained by the rotation of the fields Z and Z':

$$Z_1 = Z \cos\phi + Z' \sin\phi \, , \tag{4a}$$

$$Z_2 = -Z \sin\phi + Z' \cos\phi \, . \tag{4b}$$

Here, the mixing angle ϕ is expressed in terms of masses as:

$$\tan^2\phi = \frac{M_Z^2 - M_1^2}{M_2^2 - M_Z^2} \simeq \frac{2 M_Z \Delta M}{M_2^2} \, , \tag{5}$$

where $\Delta M = M_Z - M_1 > 0$, M_Z being the mass of the Z_1 boson in the absence of mixing, i.e., for $\phi = 0$. Once we assume the mass M_1 to be determined experimentally, the mixing depends on two free parameters, which we identify as ϕ and M_2.

In general, such mixing effects reflect the underlying gauge symmetry and/or the Higgs sector of the model. To a good approximation, for $M_1 \ll M_2$, in specific 'minimal-Higgs models',

$$\phi \simeq -s_{\rm W}^2 \, \frac{\sum_i \langle \Phi_i \rangle^2 I_{3L}^i Q_i'}{\sum_i \langle \Phi_i \rangle^2 (I_{3L}^i)^2} = \mathcal{C} \, \frac{M_1^2}{M_2^2}. \tag{6}$$

Here $\langle \Phi_i \rangle$ are the Higgs vacuum expectation values spontaneously breaking the symmetry, and Q_i' are their charges with respect to the additional $U(1)'$. In addition, in these models the same Higgs multiplets are responsible for both generation of mass M_1 and for the strength of the Z-Z' mixing. Thus $\mathcal{C}$ is a model-dependent constant. For example, in the case of E_6 superstring-inspired models $\mathcal{C}$ can be expressed as [22]

$$\mathcal{C} = 4 s_{\rm W} \left(A - \frac{\sigma - 1}{\sigma + 1} B \right), \tag{7}$$

where $s_{\rm W}$ is the sine of the electroweak angle, σ is the ratio of vacuum expectation values squared, and the constants A and B are determined by an angle β defining a direction in the extended gauge symmetry sector: $A = \cos\beta / 2\sqrt{6}$, $B = \sqrt{10}/12 \sin\beta$.

An important property of the models under consideration is that the gauge eigenstate Z' does not couple to the W^+W^- pair since it is neutral under $SU(2)_L$. Therefore the process (2) is sensitive to a Z' only in the case of a non-zero Z-Z' mixing.

From (4), one obtains the vector and axial-vector couplings of the Z_1 and Z_2 bosons to fermions:

$$v_{1f} = v_f \cos\phi + v_f' \sin\phi \ , \ a_{1f} = a_f \cos\phi + a_f' \sin\phi \ , \tag{8a}$$

$$v_{2f} = v_f' \cos\phi - v_f \sin\phi \ , \ a_{2f} = a_f' \cos\phi - a_f \sin\phi \ , \tag{8b}$$

with $(v_f, a_f) = (g_L^f \pm g_R^f)/2$, and (v_f', a_f') similarly defined in terms of the Z' couplings. The fermionic Z' couplings can be found, e.g. in [17].

Analogously, one obtains according to the remarks above:

$$g_{WWZ_1} = \cos\phi \, g_{WWZ} \ , \tag{9a}$$

$$g_{WWZ_2} = -\sin\phi \, g_{WWZ} \ , \tag{9b}$$

where $g_{WWZ} = \cot\theta_W$.

In our analysis, we ignore kinetic mixing [23]. Such mixing would introduce an additional parameter, and could modify the exclusion reach (see, for example [24, 25]).

III. CROSS SECTION

The parton model cross section for the process (2) from initial quark-antiquark states can be written as

$$\frac{d\sigma_{q\bar{q}}}{dM\,dy\,dz} = K\frac{2M}{s}\sum_{q}[f_{q|P_1}(\xi_1)f_{\bar{q}|P_2}(\xi_2) + f_{\bar{q}|P_1}(\xi_1)f_{q|P_2}(\xi_2)]\,\frac{d\hat{\sigma}_{q\bar{q}}}{dz}\,. \tag{10}$$

Here, s is the proton-proton center-of-mass energy squared; $z = \cos\theta$ with θ the W^--boson–quark angle in the W^+W^- center-of-mass frame; y is the diboson rapidity; $f_{q|P_1}(\xi_1, M)$ and $f_{\bar{q}|P_2}(\xi_2, M)$ are parton distribution functions in the protons P_1 and P_2, respectively, with $\xi_{1,2} = (M/\sqrt{s})\exp(\pm y)$ the parton fractional momenta; finally, $d\hat{\sigma}_{q\bar{q}}/dz$ are the partonic differential cross sections. In (10), the K factor accounts for next-to-leading order QCD contributions [26, 27] (for the invariant WW mass-dependent cross section, see [28, 29]). For simplicity, we will use as an approximation a global flat value $K = 1.2$ [28, 29] both for the SM and Z' boson cases. For numerical computation, we use CTEQ-6L1 parton distributions [30]. Since our estimates will be at the Born level, the factorisation scale $\mu_{\rm F}$ enters solely through the parton distribution functions, as the parton-level cross section at this order does not depend on $\mu_{\rm F}$. As regards the scale dependence of the parton distributions we choose for the factorization scale the WW invariant mass, i.e., $\mu_{\rm F}^2 = M^2 = \hat{s}$, with $\hat{s} = \xi_1\,\xi_2\,s$ the parton subprocess c.m. energy squared. We have checked that the obtained constraints presented in the following are not significantly modified when $\mu_{\rm F}$ is varied in the interval $\mu_{\rm F}/2$ to $2\mu_{\rm F}$.

Taking into account the experimental rapidity cut relevant to the LHC experiments, ($Y_{\rm cut} = 2.5$), one should carry out the integration over the phase space in (10) determined as [31, 32]:

$$|y| \leq Y = \min\left[\ln(\sqrt{s}/M), Y_{\rm cut}\right] = \ln(\sqrt{s}/M), \tag{11}$$

where we make use of the fact that we do not consider low masses, $\ln(\sqrt{s}/M) < Y_{\rm cut}$. This leads to a cut in the production angle

$$|z| \leq z_{\rm cut} = \min\left[\tanh(Y_{\rm cut} - |y|)/\beta_W, 1\right]\,, \tag{12}$$

where $\beta_W = \sqrt{1 - 4M_W^2/\hat{s}}$ and M_W is the W boson mass.

The resonant Z' production cross section of process (2) needed in order to estimate the expected number of Z' events, can be derived from (10) by integrating its right-hand-side

over z, the rapidity of the $W^{\pm}$-pair y and invariant mass M around the resonance peak $(M_R - \Delta M/2,\, M_R + \Delta M/2)$:

$$\sigma(pp \to W^+W^- + X) = \int_{M_R-\Delta M/2}^{M_R+\Delta M/2} dM \int_{-Y}^{Y} dy \int_{-z_{\rm cut}}^{z_{\rm cut}} dz \frac{d\sigma_{q\bar{q}}}{dM\, dy\, dz} \,. \tag{13}$$

We adopt the parametrization of the experimental mass resolution ΔM in reconstructing the diboson invariant mass of the W^+W^- system, ΔM vs. M, as proposed in Ref. [33]. (After integration over y, interference effects vanish.)

The parton level $W^{\pm}$ boson pair production can be described, within the gauge models discussed here, by the subprocesses

$$q\bar{q} \to \gamma, Z_1, Z_2 \to W^+W^-, \tag{14}$$

as well as t- and u-channel Feynman diagrams displayed in Fig. 1.

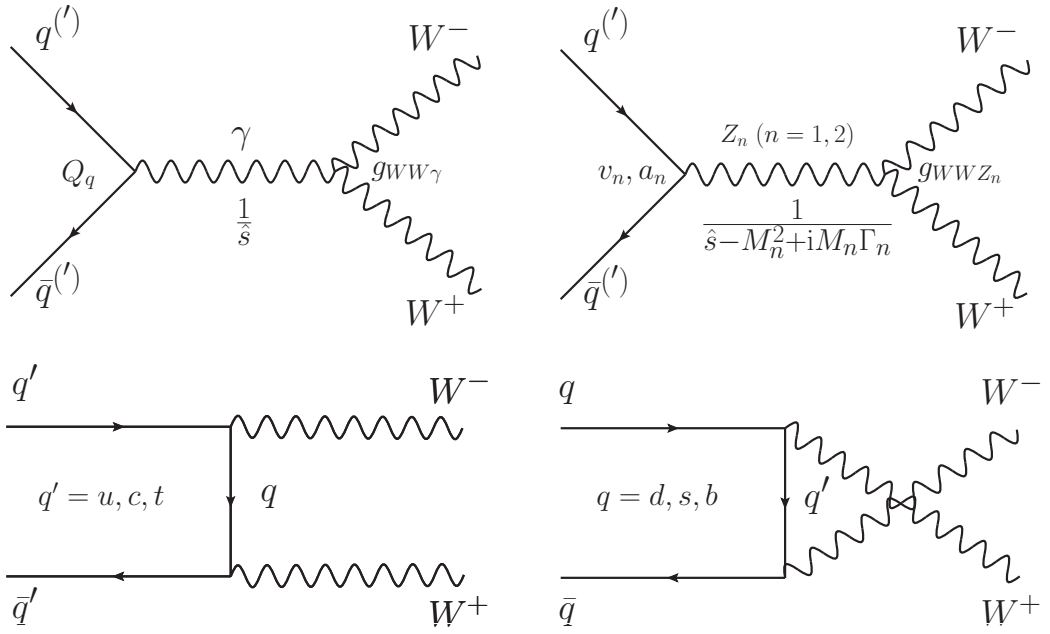

FIG. 1: Feynman diagrams of the $q\bar{q}$ $(q'\bar{q}') \to W^+W^-$ process within the framework of the extended gauge models.

The differential (unpolarized) cross section of process (14) can be written as:

$$\frac{d\hat{\sigma}_{q\bar{q}}}{dz} = \frac{1}{N_C} \frac{\beta_W}{32\pi\hat{s}} \sum_{\lambda,\lambda',\tau,\tau'} |F_{\lambda\lambda'\tau\tau'}(\hat{s},\theta)|^2 \,. \tag{15}$$

Here, N_C is the number of quark colors; $\lambda = -\lambda' = \pm 1/2$ are the quark helicities; the helicities of the W^- and W^+ are denoted by $\tau, \tau' = \pm 1, 0$. The helicity amplitudes $F_{\lambda\lambda'\tau\tau'}(\hat{s}, \theta)$ are summarized in Table I that reproduces the SM expectations if one ignores the effects of the Z-Z' mixing [31, 34, 35]. There $\hat{s}$, $\hat{t}$, $\hat{u}$ are the Mandelstam variables defined as $\hat{t} = M_W^2 - \hat{s}(1 - \beta_W z)/2$, $\hat{u} = M_W^2 - \hat{s}(1 + \beta_W z)/2$; $\Gamma_{1,2}$ are $Z_{1,2}$ boson decay widths; $g_{1,f}^{\lambda} = v_{1,f} - 2a_{1,f}\lambda$, $g_{2,f}^{\lambda} = v_{2,f} - 2a_{2,f}\lambda$; and $\gamma_W = \sqrt{\hat{s}}/2M_W$. In the t- and u-channel exchanges of Fig. 1 we account for the initial $q = u, d, s, c$, only the CKM favoured quarks in the approximation of unity relevant matrix element.

In evaluation of the total width Γ_2 of the Z_2 boson we take into account its decay channels into fermions (quarks and leptons) and $W^{\pm}$ boson pair [36]:

$$\Gamma_2 = \sum_f \Gamma_2^{ff} + \Gamma_2^{WW} \ . \tag{16}$$

Further contributions of decays involving Higgs and/or gauge bosons and supersymmetric partners (including sfermions), which are not accounted for in (16), could increase Γ_2 by a model-dependent amount typically as large as 50% [36]. For a discussion of width effects, see [37].

The fermion contribution, $\sum_f \Gamma_2^{ff}$, depends on the number n_g of generations of heavy exotic fermions which can contribute to Z_2 decay without phase space suppression (we can assume that the three known generations do contribute). This number is model dependent too, and brings a phenomenological uncertainty. For the range of M_2 values assumed here, of the order of a few TeV, the dependence of Γ_2 on ϕ induced by $\sum_f \Gamma_2^{ff}$ and by Γ_2^{WW} is unimportant. For definiteness the Z_2 width Γ_2 is assumed to scale with the Z_2 mass $\Gamma_2 = (M_2/M_1)\Gamma_1 \approx 0.03\, M_2$. This scaling is what would be expected for the reference model SSM [38]. Choosing this scaling is a conservative assumption since in E_6 models, the Z_2 width would be substantially narrower than this (see Table II).

The differential cross section for the processes $q\bar{q} \to Z' \to W^+W^-$, averaged over quark colors, can easily be obtained from Eq. (15) and written as [39]

$$\frac{d\hat{\sigma}_{q\bar{q}}^{Z'}}{d\cos\theta} = \frac{1}{3}\,\frac{\pi\alpha^2\cot^2\theta_W}{16}\beta_W^3\left(v_{2,f}^2 + a_{2,f}^2\right)\sin^2\phi\,\frac{\hat{s}}{\left(\hat{s} - M_2^2\right)^2 + M_2^2\Gamma_2^2} \times \left(\frac{\hat{s}^2}{M_W^4}\sin^2\theta + 4\frac{\hat{s}}{M_W^2}(4 - \sin^2\theta) + 12\sin^2\theta\right). \tag{17}$$

The resonant production cross section of process (2) at hadronic level can be derived from Eqs. (10) and (17).

TABLE I: Helicity amplitudes [31] of $q\bar{q} \to W^+W^-$. To obtain the amplitude $F_{\lambda\lambda'\tau\tau'}(\hat{s},\theta)$ for a definite quark helicity $\lambda = -\lambda' = \pm 1/2$ and fixed helicities $\tau(W^-)$ and $\tau'(W^+)$ of the final-state system, it is necessary to multiply each element of the respective column by the common factor in its upper part, to multiply successively the elements obtained in this way by the respective elements in the first column, and to perform thereupon summation over all intermediate states.

	helicity of $W^\pm$	$\tau = \tau' = \pm 1$	$\tau = -\tau' = \pm 1$
channel	$W_T^- W_T^+$	$-e^2\hat{s}\lambda \sin\theta/2$	$-e^2\hat{s}\lambda \sin\theta/2$
t	$\frac{2\lambda-1}{4\hat{t}s_{\rm W}^2}$	$\cos\theta - \beta_W$	$-\cos\theta - 2\tau\lambda$
u	$\frac{2\lambda-1}{4\hat{u}s_{\rm W}^2}$	$\cos\theta + \beta_W$	$-\cos\theta - 2\tau\lambda$
s	$\frac{2Q_f}{\hat{s}} + g_{1,f}^\lambda \frac{2g_{WWZ_1}}{\hat{s}-M_1^2+iM_1\Gamma_1}$ $+g_{2,f}^\lambda \frac{2g_{WWZ_2}}{\hat{s}-M_2^2+iM_2\Gamma_2}$	$-\beta_W$	0

	helicity of $W^\pm$	$\tau = \tau' = 0$	
channel	$W_L^- W_L^+$	$-e^2\hat{s}\lambda \sin\theta/2$	
t	$\frac{2\lambda-1}{4\hat{t}s_{\rm W}^2}$	$2\gamma_W^2\left(\cos\theta - \beta_W(1+\frac{1}{2\gamma_W^2})\right)$	
u	$\frac{2\lambda-1}{4\hat{u}s_{\rm W}^2}$	$2\gamma_W^2\left(\cos\theta + \beta_W(1+\frac{1}{2\gamma_W^2})\right)$	
s	$\frac{2Q_f}{\hat{s}} + g_{1,f}^\lambda \frac{2g_{WWZ_1}}{\hat{s}-M_1^2+iM_1\Gamma_1}$ $+g_{2,f}^\lambda \frac{2g_{WWZ_2}}{\hat{s}-M_2^2+iM_2\Gamma_2}$	$-\beta_W(1+2\gamma_W^2)$	

	helicity of $W^\pm$	$\tau = 0, \tau' = \pm 1$	$\tau = \pm 1, \tau' = 0$
channel	$W_L^- W_T^+ + W_T^- W_L^+$	$\frac{-e^2\hat{s}\lambda}{2\sqrt{2}}\left(\tau' \cos\theta - 2\lambda\right)$	$\frac{-e^2\hat{s}\lambda}{2\sqrt{2}}\left(\tau \cos\theta + 2\lambda\right)$
t	$\frac{2\lambda-1}{4\hat{t}s_{\rm W}^2}$	$\gamma_W\left[\cos\theta(1+\beta_W^2) - 2\beta_W\right]$ $-\frac{\tau' \sin^2\theta}{\gamma_W(\tau'\cos\theta - 2\lambda)}$	$-\gamma_W\left[\cos\theta(1+\beta_W^2) - 2\beta_W\right]$ $+\frac{\tau \sin^2\theta}{\gamma_W(\tau\cos\theta + 2\lambda)}$
u	$\frac{2\lambda-1}{4\hat{u}s_{\rm W}^2}$	$\gamma_W\left[\cos\theta(1+\beta_W^2) + 2\beta_W\right]$ $-\frac{\tau' \sin^2\theta}{\gamma_W(\tau'\cos\theta - 2\lambda)}$	$-\gamma_W\left[\cos\theta(1+\beta_W^2) + 2\beta_W\right]$ $+\frac{\tau \sin^2\theta}{\gamma_W(\tau\cos\theta + 2\lambda)}$
s	$\frac{2Q_f}{\hat{s}} + g_{1,f}^\lambda \frac{2g_{WWZ_1}}{\hat{s}-M_1^2+iM_1\Gamma_1}$ $+g_{2,f}^\lambda \frac{2g_{WWZ_2}}{\hat{s}-M_2^2+iM_2\Gamma_2}$	$-2\beta_W\gamma_W$	$2\beta_W\gamma_W$

TABLE II: Ratio Γ_2/M_2 for the χ, ψ, η and SSM models.

Z'	Γ_2/M_2 [%]
χ	1.2
ψ	0.5
η	0.6
SSM	3.0

It is important to notice that the dominant term in Eq. (17), for $M^2 \gg M_W^2$, is proportional to $(M/M_W)^4 \cdot \sin^2\theta$ and corresponds to the production of longitudinally polarized W's, $Z' \to W_L^+ W_L^-$. This increasing (with the parton sub-energy squared $\hat{s}$) behavior of the cross section in the Z' scenarios considered in Table II, would, in turn, result in a corresponding enhanced sensitivity to Z-Z' mixing at high M.

For illustrative purposes, the invariant mass distribution of $W^\pm$ pairs in the process $pp \to W^+W^+ + X$ in the SM (solid black curve) and for the $Z'_{\rm SSM}$ model at two vaues of the Z-Z' mixing angle at the LHC with $\sqrt{s} = 14$ TeV is shown in Fig. 2. The $W^\pm$-pair invariant mass distribution ($d\sigma/dM$) is calculated with the same parton distribution functions and event selection criterion as those used in Ref. [40]. Also, the bin size ΔM of the diboson invariant mass is depicted for comparison with the Z' width. For numerical computations, we take $\Delta M = 0.03M$. The W bosons are kept on-shell and their subsequent decays are not included in the crosss sections represented in Fig. 2. Here, we assumed that the invariant mass distribution of the cross section can be reconstructed from the decay products of the W^+W^-. Fig. 2 shows that at the LHC with integrated luminosity $\mathcal{L}_{\rm int} = 100$ fb^{-1} the expected number of W^+W^- background events within a mass bin ΔM is of the order of a few events while the resonant yield at $\phi = 10^{-3}$ is $N_{Z'} \sim 100$.

IV. SIGNAL AND BACKGROUNDS

In this section we focus on the WW production via intermediate Z' and subsequent purely leptonic decay of on-shell W's, that will be probed experimentally at LHC, namely:

$$pp \to WW + X \to l\nu l'\nu' + X \quad (l, l' = e \text{ or } \mu), \tag{18}$$

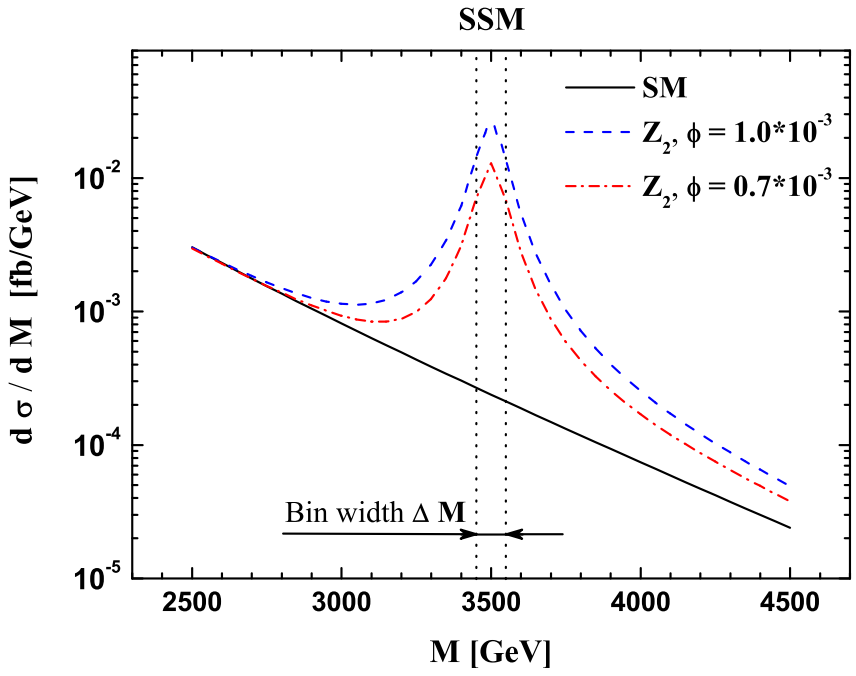

FIG. 2: Invariant mass distribution of $W^{\pm}$ pairs in $pp \to W^+W^- + X$ in the SM (solid curve) and for the $Z'_{\rm SSM}$ model ($M_{Z'} = 3.5$ TeV) with Z-Z' mixing angle of $\phi = 10^{-3}$ (dashed line) and $\phi = 0.7 \cdot 10^{-3}$ (dash-dotted line) at the LHC with $\sqrt{s} = 14$ TeV.

and, following the analysis given in [42, 43], we briefly introduce the main backgrounds and possible cuts to enhance the Z' signal to background ratio. The $WW \to \tau\nu l\nu$ and $WW \to \tau\nu\tau\nu$ processes with τ leptons decaying into electrons and muons with additional neutrinos are also included. Three final states are considered, based on the lepton flavor, namely ee, $\mu\mu$, and $e\mu$ [21]. The branching fraction of the decay channels WW into e^+e^-, $e^+\mu^-$ and $\mu^+\mu^-$ pairs can be found in Table III.

The presence of (at least) two neutrinos in the final state makes almost impossible the complete reconstruction of the WW invariant mass, so that in any case the Z' peak would be broadened. (For the pure leptonic channel discussed below, the actual final-state width will be broader [42], however this is not the case for the semileptonic channel.) For an attempt to reconstruct the M_{WW} distribution by means of estimating the momenta of escaping neutrinos, see, for example, Ref. [43]. Alternatively, a possible kinematical variable to

TABLE III: Branching fractions of the $WW \to l\nu l'\nu'$ ($l, l' = e$ or μ) decay channels [41].

process	Br [%]
$WW \to ee$	1.16
$WW \to \tau e/\tau\tau \to ee$	0.47
$WW \to e\mu$	2.27
$WW \to \tau l \to e\mu$	0.92
$WW \to \mu\mu$	1.12
$WW \to \tau\mu/\tau\tau \to \mu\mu$	0.45

characterize both the Z' signal and the background should be the transverse WW mass M_T^{WW} (a Z' would lead to an excess of events at $M_T^{WW} > M_{Z'}/2$), which has the advantage that only (measurable) transverse momenta are involved [42]. Both methods seem to lead to similar results, namely, the distributions of events are dominated by characteristic Z' bumps over the backgrounds.

A. Different-flavor leptons

In the case of different-flavor leptons ($e\mu$), the Z' signal in the process (18) possesses SM backgrounds coming from the production of W^+W^- pairs with its subsequent leptonic decay.

In order to perform effectively the detection and isolation of the final leptons with opposite charges, paralleling Ref. [42] we apply:

$$|\eta_l| < 2.5,\ \Delta R_{ll} > 0.4,\ p_T^l > 50\,\text{GeV}, \tag{19}$$

where $\Delta R_{ll} = \sqrt{(\Delta\eta)^2 + (\Delta\phi)^2}$ parametrizes the separation in rapidity η and azimuthal angle ϕ.

Apart from the SM mechanism, another potentially sizable source of background arises from $t\bar{t}$ pair production where the top quarks decay to $b + W$, leading to b-jets. This background can be efficiently reduced by vetoing the presence of additional jets with

$$|\eta_j| < 3 \quad \text{and} \quad p_T^j > 20\ \ \text{GeV}. \tag{20}$$

However, it is necessary to account for the possible appearance of an additional jet in the signal event sample, originating either from QCD gluon radiation or from the pile-up of pp interactions caused by the high luminosity. Accordingly, one can introduce probabilities for survival to the central jet veto (20) of QCD and electroweak events, and the following values are found [43]:

$$P_{\rm surv}^{\rm EW} = 0.56, \qquad P_{\rm surv}^{\rm QCD} = 0.23. \tag{21}$$

The above constraints will be included in the statistical analysis carried out in the next section. Of course, an even stronger background suppression, relative to the Z' signal, might be obtained by imposing the reconstructed WW mass to coincide within a width with the [possibly determined fron DY] Z' mass.

B. Same-flavor leptons

For same-flavor leptons (ee or $\mu\mu$) there are additional backgrounds originating from Drell-Yan lepton pair production, and from the ZZ production with one Z decaying into charged leptons and the other decaying invisibly or with both Zs decaying into charged leptons, two of which escape undetected. In this case, two extra cuts should be imposed in order to suppress the Drell–Yan pair production and ZZ background, namely

$$E_T^{\rm miss} > 50 \text{ GeV}, \quad m_{\ell^+\ell^-} > 100 \text{ GeV}, \tag{22}$$

respectively. As was concluded in [42, 43], after applying the cuts, the electroweak background originating from $t\bar{t}$ pair production at high Z' masses becomes negligible with respect to the irreducible background induced from W^+W^- pair production via the SM.

V. CONSTRAINTS ON Z'

In our analysis, we denote by $N_{\rm SM}$ and $N_{Z'}$ the numbers of 'background' and 'signal' events, and we adopt the criterion $N_{Z'} = 2\sqrt{N_{\rm SM}}$ or 3 events, whichever is larger, as the minimum signal for reach at the 95% C.L. [4]. Here, the Z' signal can be determined as

$$N_{Z'} = \mathcal{L}_{\rm int} \times \sigma^{Z'} \times P_{\rm surv}^{\rm EW} \times A \times \epsilon^{\ell}, \tag{23}$$

with

$$\sigma^{Z'} = \sigma(pp \to Z') \times {\rm Br}(Z' \to W^+W^- \to l\nu l'\nu'). \tag{24}$$

In Eq. (23), $\mathcal{L}_{\rm int}$ is the time-integrated luminosity, and $A \times \epsilon^{\ell}$ is the product of the overall acceptance times the lepton detection and reconstruction efficiencies where A represents the kinematic and geometric acceptance from the total phase space to the fiducial phase space governed by Eqs. (11) and (12), while ϵ^{ℓ} represents detector effects such as lepton trigger and identification efficiencies. The overall acceptance times the lepton efficiency is $W^{\pm}$ invariant mass dependent and, for simplicity, we take that to be 0.5. The SM background reads:

$$N_{\rm SM} = \mathcal{L}_{\rm int} \times \left(\sigma^{\rm EW}_{\rm SM} \times P^{\rm EW}_{\rm surv} + \sigma^{t\bar{t}}_{\rm SM} \times P^{\rm QCD}_{\rm surv} \right) \times A \times \epsilon^{\ell} \approx \mathcal{L}_{\rm int} \times \sigma^{\rm EW}_{\rm SM} \times P^{\rm EW}_{\rm surv} \times A \times \epsilon^{\ell}, \quad (25)$$

where $\sigma^{\rm EW}_{\rm SM}$ is determined by Eqs. (13) and (15) taking into account solely the SM contribution. Also, in the latter expression for $N_{\rm SM}$ we take into account that for heavy $M_{Z'}$, $\sigma^{\rm EW}_{\rm SM} \gg \sigma^{t\bar{t}}_{\rm SM}$ as was shown in [42].

One should notice that the latter estimation of the SM background, $\sigma^{\rm EW}_{\rm SM}$, is consistent with what is obtained by using the so-called MAOS method to reconstruct the WW invariant mass described in [43]. However, we numerically find that at high Z' mass, $M_{Z'} > 3$ TeV, the SM background becomes so low that the criterion $N_{Z'} = 3$ can be applied in obtaining constraints on Z' parameters.

A. Leptonic WW decays

We depict in Figs. 3–5 the region in parameter space to which the LHC will be able to constrain Z-Z' mixing for an integrated luminosity of 100 fb^{-1}.

In particular, the discovery reach on the Z-Z' mixing and M_2 mass for $Z'_{\rm SSM}$ obtained from the process $pp \to WW + X \to l\nu l'\nu' + X$ ($l, l' = e$ or μ) at the LHC with $\sqrt{s} = 14$ TeV and $\mathcal{L}_{\rm int} = 100$ fb^{-1} are depicted by the two solid lines. The form of these bounds is governed by the criterion of $N_{Z'} = 3$ and the quadratic dependence of the resonant cross section, Eq. (17), on the Z-Z' mixing angle. Also, current limits on M_2 for $Z'_{\rm SSM}$ derived from the Drell–Yan (l^+l^-) process at the LHC (8 TeV) (horizontal solid line) as well as those expected from the future experiments at the LHC with 14 TeV (horizontal dotted line) are shown. The combined allowed area in the (ϕ, M_2) plane obtained from the Drell–Yan and $W^{\pm}$ pair production processes is shown as a hatched region. In addition, present limits on the Z-Z' mixing angle obtained from electroweak precision data analysis [10] labelled as 'EW data' are displayed (these have a weak mass dependence which we have not attempted to

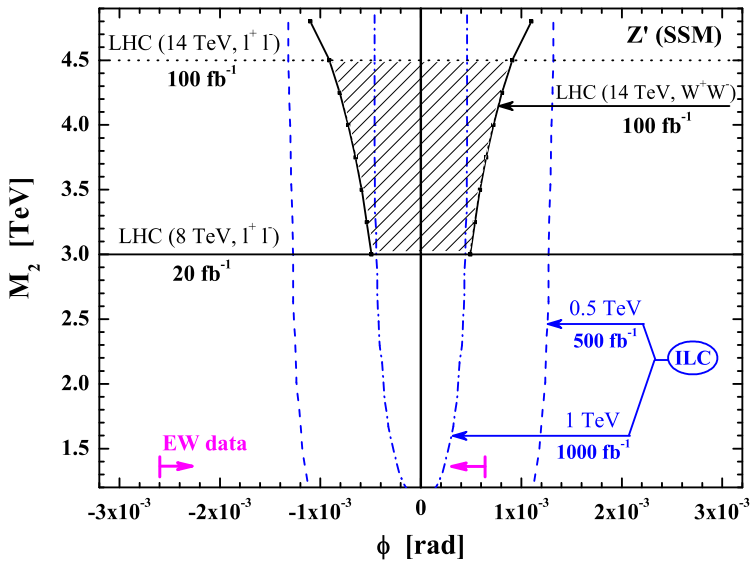

FIG. 3: Reach (at 95 %C.L.) on Z-Z' mixing and M_2 mass for $Z'_{\rm SSM}$ obtained from the inclusive process $pp \to WW \to l\nu l'\nu'$ ($l, l' = e$ or μ) at the LHC (solid lines). The allowed domain in ϕ and M_2 is the hatched one. Current limits on M_2 for $Z'_{\rm SSM}$ derived from the Drell–Yan (l^+l^-) process at the LHC (8 TeV) (horizontal solid line) as well as 'typical' mass limits expected at the LHC (14 TeV) (horizontal dotted line) are shown. Limits on the Z-Z' mixing angle from electroweak precision data are displayed, and those expected from $W^\pm$ pair production at the ILC with polarized beams.

draw). For comparison, the corresponding limits obtained from $W^\pm$ pair production at the ILC with polarized beams and for two options of energy and time-integrated luminosity (0.5 (1) TeV and 0.5 (1) ab^{-1}, respectively) are also presented [17]. Figs. 3–5 show that the LHC is able to not only significantly improve the current limits on the Z-Z' mixing angle, but in several cases, also allow more stringent bounds than those expected from future experiments on the WW channel at the electron–positron collider ILC [11].

In Fig. 6 we return to the $Z'_{\rm SSM}$ and show the sensitivity reach (at 95 %C.L.) on the Z-Z' mixing and M_2 mass obtained from the W pair production process at the LHC with $\sqrt{s} = 8$ TeV and $\mathcal{L}_{\rm int} = 20$ fb^{-1} under the assumption that no significant excess in the overall number of WW events is observed in the data. $Z' \to WW$ effects at the 8 TeV LHC with a luminosity of 4.8 fb^{-1} have been discussed in [44–47].[1] The form of these bounds reflects

[1] Recent studies [48, 49] claim a small excess compatible with stop production and decay.

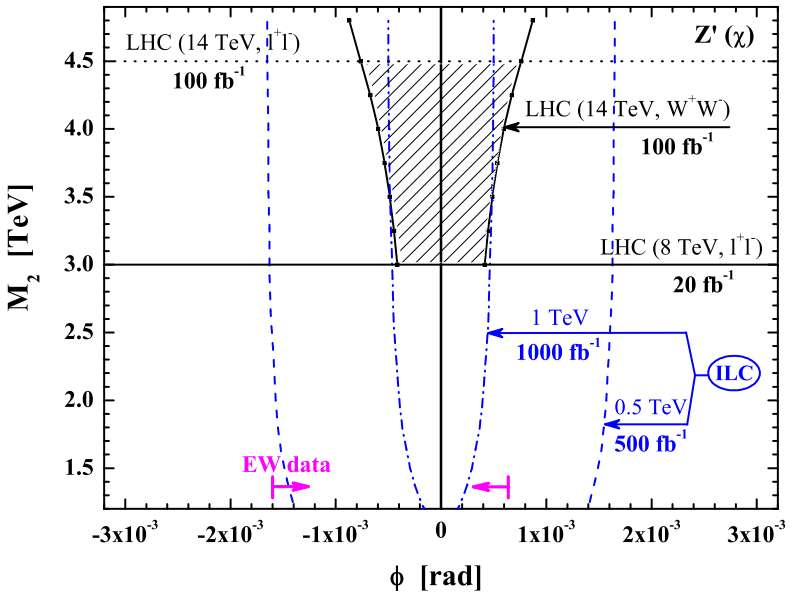

FIG. 4: Same as in Fig. 3 but for Z'_χ.

the fact that the number of background events is below 3, and that the criterion $N_{Z'} < 3$ is the crucial one. For comparison, also the results for 14 TeV and 100 fb^{-1} (shown in Fig. 3) are included, together with current limits on M_2 derived from the Drell–Yan process, $pp \to l^+l^- + X$, at 8 TeV, and constraints from electroweak data. Fig. 6 shows that the current limits on ϕ from the EW precision data are stronger than those obtained from the present LHC data collected from the 8 TeV run, while the LHC with 14 TeV possesses a high potential to substantially improve the current bounds on the Z-Z' mixing angle.

B. Semileptonic WW decays

As mentioned above, another process where one can search for a new diboson resonance such as the Z' is represented by the subsequent WW decay into an $l\nu jj$ final state, i.e., a charged lepton (electron or muon), large missing transverse momentum ($E_T^{\rm miss}$), and at least two jets,

$$pp \to WW + X \to l\nu jj + X. \tag{26}$$

An advantage of that process is that it has a higher crosss section with respect to the pure leptonic final states. Also, the $l\nu jj$ final state allows the reconstruction of the invariant mass

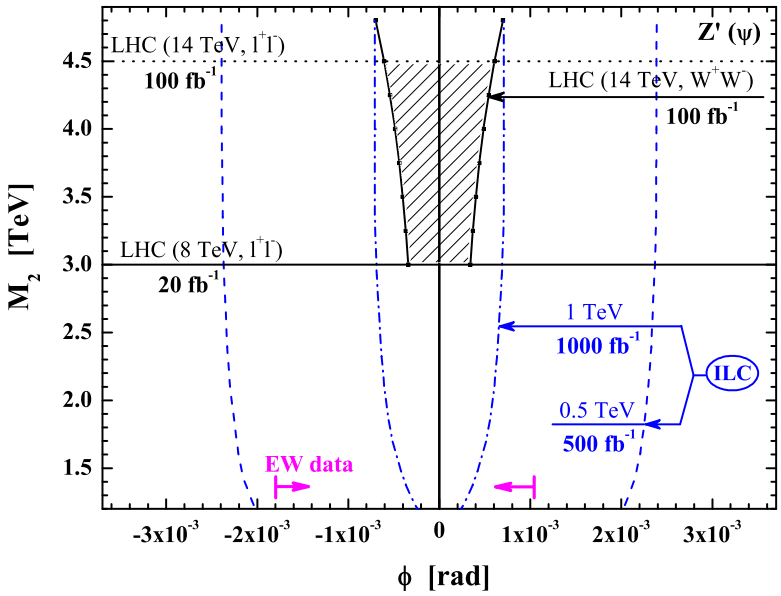

FIG. 5: Same as in Fig. 3 but for Z'_ψ.

of the WW system, under certain assumptions for the neutrino longitudinal momentum from a W boson decay. As a result, a sharper Z' signal can be obtained. On the other hand, this channel has large QCD backgrounds due to the Wjj production, as well as Zjj with Z decaying leptonically and one of the leptons being missed. Also, $t\bar{t}$ production contributes to the background. However, the large QCD background can be reduced by making use of the characteristic harder transverse momenta of the charged lepton and the jets in the Z' signal. A detailed analysis of the QCD background and the corresponding cuts imposed, resulting in its substantial reduction, the estimation on the discovery potential of the Z' boson in this channel is given in [38] and, more recently, in [42]. For the overall background we refer to Ref. [38] in our further analysis, in order to quantify the expected statistical significance as a function of $M_{Z'}$ for different Z' models. We find that for the integrated luminosity of 100 fb^{-1} the semileptonic channel allows to make further improvement of the current limits on the Z-Z' mixing angle as reported in Fig. 7 and summarized in Table IV.

In Fig. 7 we also show the ϕ–M_2 relation for the specific 'minimal-Higgs model' determined by Eq. (6) where $\mathcal{C}$ is chosen to be unity [38, 50]. The possibility of the Z' boson detection in the semileptonic decay mode of WW at the LHC has been discussed in [38]. Our numerical results for this model presented in Fig. 7 are consistent with those given in Ref. [38]. However,

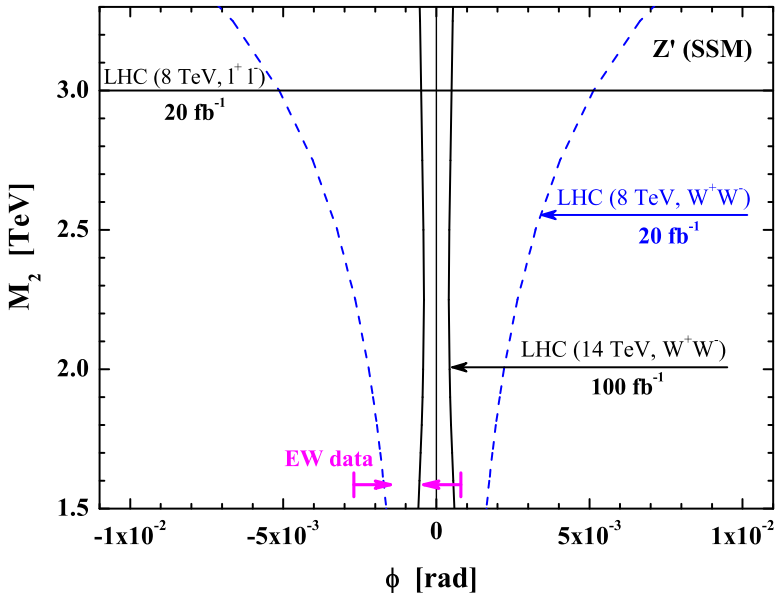

FIG. 6: Reach (at 95 %C.L.) on Z-Z' mixing and M_2 mass for $Z'_{\rm SSM}$ obtained from the inclusive process $pp \to WW \to l\nu l'\nu'$ at the LHC with $\sqrt{s} = 8$ TeV and $\mathcal{L}_{\rm int} = 20$ fb^{-1} (dashed curves) and $\sqrt{s} = 14$ TeV and $\mathcal{L}_{\rm int} = 100$ fb^{-1} (solid curves). Also shown are current limits on M_2 derived from the Drell–Yan process at the LHC (8 TeV) denoted by the label l^+l^- and constraints from electroweak precision data. Note that the scale is different from that of Figs. 3–5.

an improvement with respect to the EW data is for the reference model only possible for negative values of ϕ.

VI. CONCLUDING REMARKS

In Table IV, we collect our limits on the Z' parameters for the models listed in Section II. Also shown in Table IV are the current limits on various Z' boson masses from the LEP2 and Tevatron from studies of diboson W^+W^- pair production. The limits on ϕ and M_2 at the Tevatron assume that no decay channels into exotic fermions or superpartners are open to the Z'. Otherwise, the limits would be moderately weaker. LEP2 constrains virtual and Z-Z' boson mixing effects by the angular distribution of W bosons. Table IV shows that the limits on ϕ from the EW precision data are generally competitive with and in many cases stronger than those from the colliders, except for the ILC (1 TeV) and LHC (14 TeV)

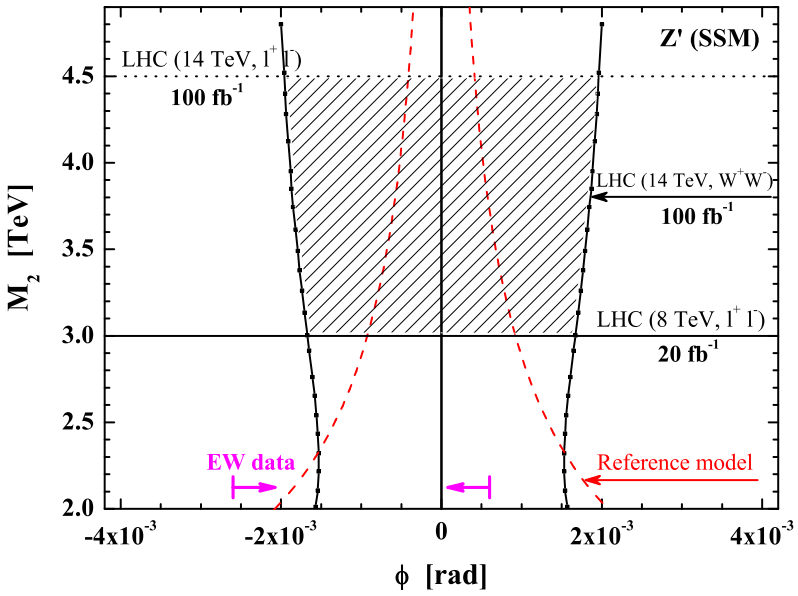

FIG. 7: Same as in Fig. 3 but obtained from the process $pp \to WW \to l\nu jj + X$ at the LHC with $\sqrt{s} = 14$ TeV and $\mathcal{L}_{\rm int} = 100$ fb^{-1}. The dashed red line shows the predicted relation between ϕ and M_2, given by Eq. (6) for the model of Ref. [50]. Note that the scale is different from those of Figs. 3–6.

that possess high potential to improve substantially the current bounds on the Z-Z' mixing angle. We stress that these limits are highly complementary.

The diboson-channel limit for $Z'_{\rm LR}$ bosons from the LHC are numerically very similar to those for the Z'_χ model, only slightly lower (not shown).

If a new Z' boson exists in the mass range $\sim$ 3–4.5 TeV, its discovery is possible in the Drell–Yan channel. Moreover, the detection of the $Z' \to W^+W^-$ mode is eminently possible and gives valuable information on the Z-Z' mixing. It might be the only mode other than the dileptonic one, $Z' \to l^+l^-$, that is accessible. Our results demonstrate that it might be possible to detect a new heavy Z' boson from the totally leptonic or semileptonic WW channels at the LHC. The LHC at nominal energy and integrated luminosity provides the best opportunity of studying a new heavy Z' through its WW decay mode and creates the possibility of measuring (or constraining) the Z-Z' mixing, thus providing insight into the pattern of symmetry breaking.

TABLE IV: Reach on the Z-Z' mixing angle ϕ at 95% C.L. in different processes and experiments.

collider, process	$\lvert\phi\rvert$	Z'_χ	Z'_ψ	Z'_η	$Z'_{\rm SSM}$	@ $M_{Z'}$
LEP2, $e^+e^- \to W^+W^-$ [11]	$\lvert\phi\rvert, 10^{-2}$	6	15	50	7	≥ 1 TeV
Tevatron, $p\bar{p} \to W^+W^- + X$ [12]	$\lvert\phi\rvert, 10^{-2}$	–	–	–	2	0.4–0.9 TeV
electroweak (EW) data [10]	$\lvert\phi\rvert, 10^{-3}$	1.6	1.8	4.7	2.6	–
ILC (0.5 TeV), $e^+e^- \to W^+W^-$ [17]	$\lvert\phi\rvert, 10^{-3}$	1.5	2.3	1.6	1.2	≥ 3 TeV
ILC (1.0 TeV), $e^+e^- \to W^+W^-$ [17]	$\lvert\phi\rvert, 10^{-3}$	0.4	0.6	0.5	0.3	≥ 3 TeV
LHC (8 TeV), $pp \to W^+W^- \to l\nu l'\nu'$ (this work)	$\lvert\phi\rvert, 10^{-3}$	–	–	–	5.2	3 TeV
LHC (14 TeV), $pp \to W^+W^- \to l\nu jj$ (this work)	$\lvert\phi\rvert, 10^{-3}$	1.7	1.2	1.1	1.7	3 TeV
LHC (14 TeV), $pp \to W^+W^- \to l\nu l'\nu'$ (this work)	$\lvert\phi\rvert, 10^{-3}$	0.4–0.8	0.3–0.6	0.3–0.6	0.5–0.9	3–4.5 TeV

Acknowledgments

It is a pleasure to thank F. Staub for pointing out the importance of kinetic mixing. This research has been partially supported by the Abdus Salam ICTP (TRIL Programme), the Collaborative Research Center SFB676/1-2006 of the DFG at the Department of Physics of the University of Hamburg and the Belarusian Republican Foundation for Fundamental Research. The work of PO has been supported by the Research Council of Norway.

[1] J. Beringer *et. al.* (Particle Data Group), Phys. Rev. D **86**, 010001 (2012).

[2] J. L. Hewett and T. G. Rizzo, Phys. Rept. **183**, 193 (1989).

[3] P. Langacker, Rev. Mod. Phys. **81**, 1199-1228 (2009) [arXiv:0801.1345 [hep-ph]].

[4] A. Leike, Phys. Rept. **317**, 143-250 (1999) [hep-ph/9805494].

[5] A. Gulov and V. Skalozub, Int. J. Mod. Phys. A **25**, 5787 (2010) [arXiv:1009.2320 [hep-ph]].

[6] S. Chatrchyan *et al.* [CMS Collaboration], Phys. Lett. B **720**, 63 (2013) [arXiv:1212.6175 [hep-ex]].

[7] G. Aad *et al.* [ATLAS Collaboration], JHEP **1211**, 138 (2012) [arXiv:1209.2535 [hep-ex]].

[8] G. Aad *et al.* [ATLAS Collaboration], arXiv:1405.4123 [hep-ex].

[9] CMS Collaboration [CMS Collaboration], CMS-PAS-EXO-12-061.

[10] J. Erler, P. Langacker, S. Munir, E. Rojas, JHEP **0908**, 017 (2009) [arXiv:0906.2435 [hep-ph]].

[11] V. V. Andreev and A. A. Pankov, Phys. Atom. Nucl. **75**, 76 (2012) [Yad. Fiz. **75**, 67 (2012)].

[12] T. Aaltonen *et al.* [CDF Collaboration], Phys. Rev. Lett. **104**, 241801 (2010) [arXiv:1004.4946 [hep-ex]].

[13] S. Schael *et al.* [ALEPH and DELPHI and L3 and OPAL and SLD and LEP Electroweak Working Group and SLD Electroweak Group and SLD Heavy Flavour Group Collaborations], Phys. Rept. **427**, 257 (2006) [hep-ex/0509008].

[14] S. Godfrey and T. Martin, arXiv:1309.1688 [hep-ph].

[15] M. Dittmar, A. -S. Nicollerat and A. Djouadi, Phys. Lett. B **583**, 111 (2004) [hep-ph/0307020].

[16] T. G. Rizzo, [hep-ph/0610104].

[17] V. V. Andreev, G. Moortgat-Pick, P. Osland, A. A. Pankov and N. Paver, Eur. Phys. J. C **72**, 2147 (2012) [arXiv:1205.0866 [hep-ph]].

[18] B. Ananthanarayan, M. Patra and P. Poulose, JHEP **1102**, 043 (2011) [arXiv:1012.3566 [hep-ph]].

[19] V. M. Abazov *et al.* [D0 Collaboration], Phys. Rev. Lett. **107**, 011801 (2011) [arXiv:1011.6278 [hep-ex]].

[20] G. Aad *et al.* [ATLAS Collaboration], Phys. Rev. D **87**, no. 11, 112006 (2013) [arXiv:1305.0125 [hep-ex]].

[21] G. Aad *et al.* [ATLAS Collaboration], Phys. Lett. B **718**, 860 (2013) [arXiv:1208.2880 [hep-ex]].

[22] P. Langacker and M. -x. Luo, Phys. Rev. D **45**, 278 (1992).

[23] B. Holdom, Phys. Lett. B **166**, 196 (1986).

[24] M. E. Krauss, B. O'Leary, W. Porod and F. Staub, Phys. Rev. D **86**, 055017 (2012) [arXiv:1206.3513 [hep-ph]].

[25] M. Hirsch, W. Porod, L. Reichert and F. Staub, Phys. Rev. D **86**, 093018 (2012) [arXiv:1206.3516 [hep-ph]].

[26] J. M. Campbell and R. K. Ellis, Phys. Rev. D **60**, 113006 (1999) [hep-ph/9905386].

[27] J. M. Campbell, R. K. Ellis and C. Williams, JHEP **1107**, 018 (2011) [arXiv:1105.0020 [hep-ph]].

[28] N. Agarwal, V. Ravindran, V. K. Tiwari and A. Tripathi, Phys. Rev. D **82**, 036001 (2010)

[arXiv:1003.5450 [hep-ph]].

[29] Y. -M. Bai, L. Guo, X. -Z. Li, W. -G. Ma and R. -Y. Zhang, Phys. Rev. D **85**, 016008 (2012) [arXiv:1112.4894 [hep-ph]].

[30] J. Pumplin, D. R. Stump, J. Huston, H. L. Lai, P. Nadolsky and W. K. Tung, JHEP **0207**, 012 (2002) [arXiv:hep-ph/0201195].

[31] E. Nuss, Z. Phys. C **76**, 701 (1997).

[32] P. Osland, A. Pankov, N. Paver, A. Tsytrinov, Phys. Rev. D **78**, 035008 (2008).

[33] ATLAS Collaboration, Reports No. CERN-LHCC-99-14, CERN-LHCC-99-15.

[34] G. Gounaris, J. Layssac, G. Moultaka and F. M. Renard, Int. J. Mod. Phys. A **8**, 3285 (1993).

[35] G. J. Gounaris and F. M. Renard, arXiv:1309.3177 [hep-ph].

[36] A. A. Pankov and N. Paver, Phys. Rev. D **48**, 63 (1993).

[37] E. Accomando, D. Becciolini, A. Belyaev, S. Moretti and C. Shepherd-Themistocleous, JHEP **1310**, 153 (2013) [arXiv:1304.6700 [hep-ph]].

[38] D. Benchekroun, C. Driouichi and A. Hoummada, Eur. Phys. J. direct C **3**, N3 (2001).

[39] F. del Aguila, L. Ametller, R. D. Field and L. Garrido, Phys. Lett. B **201**, 375 (1988).

[40] N. Agarwal, V. Ravindran, V. K. Tiwari and A. Tripathi, Phys. Lett. B **690**, 390 (2010) [arXiv:1003.5445 [hep-ph]].

[41] M. P. Cooke, "WW production cross section measurement and limits on anomalous trilinear gauge couplings at $\sqrt{s} = 1.96$ TeV", Thesis, Rice University, Houston, Texas, 2008, 163 pages.

[42] A. Alves, O. J. P. Eboli, D. Goncalves, M. C. Gonzalez-Garcia and J. K. Mizukoshi, Phys. Rev. D **80**, 073011 (2009) [arXiv:0907.2915 [hep-ph]].

[43] O. J. P. Eboli, C. S. Fong, J. Gonzalez-Fraile and M. C. Gonzalez-Garcia, Phys. Rev. D **83**, 095014 (2011) [arXiv:1102.3429 [hep-ph]].

[44] J. Gonzalez-Fraile, arXiv:1205.5802 [hep-ph].

[45] O. J. P. Eboli, J. Gonzalez-Fraile and M. C. Gonzalez-Garcia, Phys. Rev. D **85**, 055019 (2012) [arXiv:1112.0316 [hep-ph]].

[46] G. Aad *et al.* [ATLAS Collaboration], Phys. Rev. D **87**, no. 11, 112001 (2013) [Erratum-ibid. D **88**, no. 7, 079906 (2013)] [arXiv:1210.2979 [hep-ex]].

[47] S. Chatrchyan *et al.* [CMS Collaboration], Eur. Phys. J. C **73**, 2610 (2013) [arXiv:1306.1126 [hep-ex]].

[48] D. Curtin, P. Meade and P. J. Tien, arXiv:1406.0848 [hep-ph].

[49] J. S. Kim, K. Rolbiecki, K. Sakurai and J. Tattersall, arXiv:1406.0858 [hep-ph].

[50] G. Altarelli, B. Mele and M. Ruiz-Altaba, Z. Phys. C **45**, 109 (1989) [Erratum-ibid. C **47**, 676 (1990)].